JOURNAL OF SOLID STATE CHEMISTRY 9, 247–254 (1974)

Structural Studies in the Li_2MoO_4–MoO_3 System: Part 1

The Low Temperature Form of Lithium Tetramolybdate, L–$Li_2Mo_4O_{13}$

B. M. GATEHOUSE* AND B. K. MISKIN

Chemistry Department, Monash University, Clayton 3168, Australia

Received May 29, 1973

L-$Li_2Mo_4O_{13}$ crystallizes in the triclinic system with unit-cell dimensions $a = 8.578$ Å, $b = 11.450$ Å, $c = 8.225$ Å, $\alpha = 109.24°$, $\beta = 96.04°$, $\gamma = 95.95°$ and space group $P\bar{1}, Z = 3$. The calculated and measured densities are 4.02 g/cm^3 and 4.1 g/cm^3 respectively. The structure was solved using three-dimensional Patterson and Fourier techniques. Of the 2468 unique reflections collected by counter methods, 1813 with $I \geqslant 3\sigma(I)$ were used in the least-squares refinement of the model to a conventional R of 0.031 ($\omega R = 0.038$). L-$Li_2Mo_4O_{13}$ is a derivative of the V_6O_{13} structure with oxygen ions arranged in a face-centred cubic type array with octahedrally coordinated molybdenum and lithium ions ordered into layers.

Introduction

The system Li_2MoO_4–MoO_3 has been studied by a number of workers. The earliest work by Hoermann (*1*) suggested the existence of three incongruently melting phases, $Li_2Mo_2O_7$, $Li_2Mo_3O_{10}$, and $Li_2Mo_4O_{13}$. Both of the more recent studies by Brower, Parker, Roth, and Waring (*2*) and Parmentier, Reau, Fouassier, and Gleitzer (*3*) agree that no compound of composition $Li_2Mo_3O_{10}$ is formed and that the compound $Li_2Mo_4O_{13}$ does exist. However, they disagree on the composition of the remaining phase which forms in the region 50–60 mol % MoO_3. Parmentier and co-workers report this phase as the dimolybdate, $Li_2Mo_2O_7$, while Brower et al. give its composition as $Li_4Mo_5O_{17}$. Brower et al. also report two polymorphic forms of $Li_2Mo_4O_{13}$; a low temperature and supposedly metastable form (L–$Li_2Mo_4O_{13}$), and a high temperature phase (H–$Li_2Mo_4O_{13}$).

Structural studies of $Li_4Mo_5O_{17}$($Li_2Mo_2O_7$) and H–$Li_2Mo_4O_{13}$, the crystals of which were kindly supplied by R. S. Roth, are currently being carried out in this laboratory. The purpose of this paper is to report the crystal structure of L–$Li_2Mo_4O_{13}$.[1] The structure was solved to enable the eventual comparison of the two polymorphs and also to compare its structure with other transition metal oxides, in particular $K_2Mo_4O_{13}$ (*4*) which has a structure composed of chains of molybdenum–oxygen octahedra held together by potassium ions. Within the molybdenum–oxygen framework the oxygens are in a face-centred cubic array, but the overall packing is disrupted by the large alkali metal ions. Lithium, however, is small enough to fit into an octahedral or tetrahedral hole and may be expected to cause minimal disruption to the packing of the oxygens. The structure of L–$Li_2Mo_4O_{13}$ may, therefore, be more easily related to other structure types which are themselves based on close-packed oxygen arrays. As the following report shows, this was found to be the case.

Experimental

Slow cooling of a melt of a mixture of lithium carbonate and molybdenum trioxide in the mole ratio 1:4 produced pale green, platy crystals of L–$Li_2Mo_4O_{13}$. The density of a representative sample of the product was measured pycnometrically and is reported in Table I. A small crystal with dimensions 0.04 × 0.05 × 0.06 mm was selected for diffraction studies, examined under a polarizing microscope for twinning and

---

[*] A preliminary communication of this structure was presented in Ref. 5.

Copyright © 1974 by Academic Press, Inc.
All rights of reproduction in any form reserved.
Printed in Great Britain

TABLE I

CRYSTALLOGRAPHIC DATA FOR L-$Li_2Mo_4O_{13}$[a]

Symmetry: Triclinic	
Space Group: $P\bar{1}$	
a: 8.578 (5) Å	α: 109.24 (7)°
b: 11.450 (5) Å	β: 96.04 (7)°
c: 8.225 (5) Å	γ: 95.95 (7)°
V: 750 (1) Å^3	Z: 3
D_c: 4.02 (1) g cm^{-3}	D_m: 4.1 (1) g cm^{-3}
μ_c: 428.6 cm^{-1}	

[a] Figures in parentheses are estimated standard deviations.

other defects and mounted about the a-axis. A preliminary Weissenberg photographic study using nickel-filtered copper radiation showed the compound to be triclinic and gave cell parameters of sufficient accuracy to be used in the subsequent alignment of the crystal on the diffractometer.

All data were collected on a Picker Nuclear FACS I four circle diffractometer (by courtesy of Dr. G. B. Robertson, Research School of Chemistry, Australian National University) using graphite monochromated, CuK_α radiation. A least-squares refinement of cell and orientation parameters using twelve high angle reflections gave the cell dimensions reported in Table I.

A $\theta - 2\theta$ scan technique with a scan width of 1.3° and allowance for dispersion was used to collect intensity data. Three non-coplanar standard reflections were measured after every fifty reflections and there appeared to be no systematic variation in their intensities. For each reflection a ten second background count was measured at both the upper and lower limits of the scan range. 2468 reflections with positive 1 index and $127° \geqslant 2\theta \geqslant 3°$ were measured. Of these only the 1813 reflections with intensity greater than three standard deviations of the intensity, and small differences between the two background counts ($|B_1 - B_2| < 3\sigma(B_1 + B_2)$) were used in the structure solution and refinement.

The usual corrections for the Lorentz and polarization effects were applied to the data. Since the plane of reflection of the graphite monochromator was perpendicular to that of the specimen, the Lorentz-polarization (Lp) correction was:

$$(\mathrm{Lp})^{-1} = \sin 2\theta(1 + \cos^2 2\theta_\mathrm{m})/(\cos^2 2\theta + \cos^2 2\theta_\mathrm{m}),$$

where $\theta_\mathrm{m} = 13.252°$ is the Bragg angle of the monochromator. The standard deviations associated with the data were calculated as follows:

$$\sigma(F) = \surd[((C + \tau^2 B)^2 + 0.001I^2)/(\mathrm{Lp})^2 \cdot 2 \cdot F],$$

where C is the peak count, B is the sum of the background counts, τ is the ratio of count time over background time, I is the net intensity $(C - \tau B)$ and F is the structure amplitude obtained from the observed intensities.

The scattering curves used in the structure factor calculations were those of Thomas and Umeda (*6*) for Mo° and Cromer and Waber (*7*) for Li^+ and O°. The Mo° curve was corrected for the real part of anomalous dispersion using the f' values given by Dauben and Templeton (*8*).

All computing was performed on the Monash University CDC 3200 and the C.S.I.R.O. CDC 3600 computers. The major programs used were MONLS, a modified version of the full-matrix least-squares program of Busing, Martin, and Levy (*9*), MONDLS, a block-diagonal least-squares program adapted from the SF series of Shiono (*10*) and the Fourier summation program of White, MONFR (*11*).

Structure solution and refinement

The solution of the structure was obtained using the P1 method described by Gatehouse and Leverett (*12*). Twelve molybdenum positions were readily found and an examination of this P1 model revealed a centre of symmetry. The six molybdenum positions in the asymmetric unit of the centrosymmetric model were then subjected to two cycles of refinement using the full-matrix least-squares technique, which reduced the conventional R to 0.166. At this stage all twenty oxygen positions were located in a difference Fourier synthesis and a least-squares refinement of the molybdenum and oxygen positions gave an R of 0.096. Fourier and difference Fourier syntheses were calculated and the three lithium positions were unambiguously located. Refinement of all positions and isotropic temperature factors reduced R to 0.039.

In subsequent refinement the data were assigned weights of $1/6^2(F)$. Successive cycles of block-diagonal least-squares refinement of all positional and thermal parameters, with anisotropic temperature factors for molybdenum and isotropic temperature factors for oxygen and lithium, caused a further drop in the conventional R to 0.031 and a reduction in the weighted

TABLE II

FINAL ATOMIC PARAMETERS WITH THEIR ESTIMATED STANDARD DEVIATIONS IN PARENTHESES

(a) Atoms with anisotropic temperature factors

Atom	x/a	y/b	z/c	U_{11}^{a}	U_{22}	U_{33}	U_{12}	U_{13}	U_{23}
Mo(1)	0.4370(2)	0.6349(1)	0.1128(2)	0.0072(6)	0.0077(6)	0.0105(6)	0.0021(5)	0.0024(5)	0.0025(5)
Mo(2)	0.4180(2)	0.6343(1)	0.5053(2)	0.0066(6)	0.0078(6)	0.0099(6)	0.0022(5)	0.0018(5)	0.0015(5)
Mo(3)	0.2095(2)	0.3591(1)	0.5320(2)	0.0057(6)	0.0076(6)	0.0101(6)	0.0006(5)	0.0015(5)	0.0021(5)
Mo(4)	0.2290(2)	0.3672(1)	0.1443(2)	0.0067(6)	0.0079(6)	0.0100(6)	0.0006(5)	0.0010(5)	0.0016(5)
Mo(5)	0.1583(2)	0.9700(1)	0.3548(2)	0.0075(6)	0.0096(6)	0.0119(6)	0.0022(5)	0.0024(5)	0.0031(5)
Mo(6)	0.1770(2)	0.9648(1)	0.9580(2)	0.0081(6)	0.0102(6)	0.0109(6)	0.0032(5)	0.0018(5)	0.0016(5)

(b) Atoms with isotropic temperature factors

Atom	x/a	y/b	z/c	B	Atom	x/a	y/b	z/c	B
O(1)	0	0	0.5	1.6(3)	O(13)	0.2902(13)	0.0009(10)	0.1853(14)	1.4(2)
O(2)	0.0052(13)	0.9935(10)	0.1511(13)	1.3(2)	O(14)	0.3284(14)	0.0058(10)	0.5042(14)	1.7(2)
O(3)	0.0772(13)	0.3982(10)	0.0200(14)	1.6(2)	O(15)	0.3259(13)	0.0016(10)	0.8544(14)	1.8(2)
O(4)	0.1066(12)	0.3892(9)	0.3344(13)	0.9(2)	O(16)	0.4085(12)	0.4178(9)	0.0376(13)	1.1(2)
O(5)	0.0796(13)	0.4024(10)	0.6780(14)	1.6(2)	O(17)	0.3966(12)	0.4021(9)	0.3755(13)	1.1(2)
O(6)	0.1275(14)	0.8113(11)	0.2775(15)	2.0(2)	O(18)	0.4126(12)	0.3852(9)	0.6714(13)	1.2(2)
O(7)	0.1445(14)	0.8067(11)	0.8802(15)	1.9(2)	O(19)	0.4830(13)	0.7909(10)	0.1975(14)	1.8(2)
O(8)	0.2254(13)	0.2119(10)	0.0701(14)	1.6(2)	O(20)	0.4335(14)	0.7900(10)	0.5866(15)	1.8(2)
O(9)	0.1776(13)	0.2000(10)	0.4513(14)	1.6(2)	Li(1)	0.0786(37)	0.6330(28)	0.1870(39)	2.0(5)
O(10)	0.2966(12)	0.5899(9)	0.2744(13)	1.0(2)	Li(2)	0.1202(33)	0.6272(25)	0.7746(35)	1.3(5)
O(11)	0.2714(13)	0.5793(10)	0.6069(14)	1.4(2)	Li(3)	0.4837(34)	0.0014(26)	0.7031(36)	1.3(5)
O(12)	0.2715(13)	0.6122(10)	0.9655(14)	1.3(2)					

[a] The anisotropic temperature factor is of the form:

$$\exp[-2\pi^2(U_{11}h^2a^{*2} + U_{22}k^2b^{*2} + U_{33}l^2c^{*2} + 2U_{12}hka^*b^* + 2U_{13}hla^*c^* + 2U_{23}klb^*c^*)].$$

R ($\omega R = \sqrt{(\sum \omega(F_0 - F_c)^2/\sum \omega F_0{}^2)}$) from 0.047 to 0.038. While none of the thermal parameters were negative, some of the isotropic temperature factors of the refined model were quite low and there appeared to be quite large variations between the principal axes of the molybdenum thermal ellipsoids. A spherical absorption correction ($\mu\bar{R} = 1.07$) was applied to the data. Although this correction was only very approximate and the effects of differential absorption were not eliminated, the refinement of all parameters, which made no change to the final R factors, did result in considerable improvement of the thermal parameters. The final parameter shifts were less than 0.1 σ and a difference Fourier synthesis calculated after the final cycle showed no maxima $>1.4\ e\text{Å}^{-3}$ and no minima $<1.6\ e\text{Å}^{-3}$. That is, there were no features on the difference map with amplitude greater than about 0.3 times the density due to a lithium atom in the Fourier synthesis.

The final parameters with their estimated standard deviations are presented in Table II. The reflections not used in the refinement were included in a final calculation of structure factors which gave a conventional R of 0.051.[2]

Description of the structure

L–$Li_2Mo_4O_{13}$ is a regular derivative structure (*13*) of V_6O_{13} (*14*) where the vanadium of the basic structure is replaced, in the derivative structure, by molybdenum and lithium. The structure is best described as a face-centred cubic array of oxygen atoms with two of every fifteen oxygen sites unoccupied and with molybdenum and lithium filling all the remaining octahedral sites in a strictly ordered manner. The idealized

---

[2] A table of observed and calculated structure factors has been deposited as Document No. NAPS-02270 with the ASIS National Auxiliary Publications Service, c/o Microfiche Publications, 305 East 46 Street, New York, N.Y. 10017. A copy may be secured by citing the document number and by remitting $5.00 for photocopies or $1.50 for microfiche. Advance payment is required. Make check or money order payable to ASIS-NAPS.

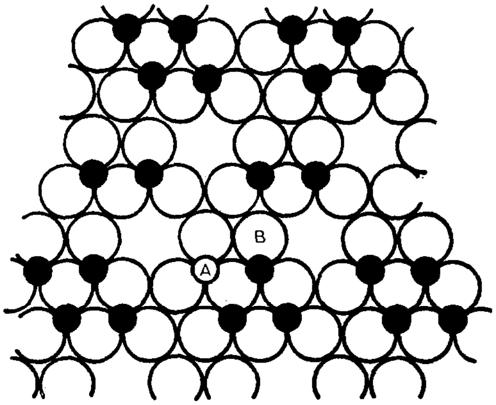

FIG. 1. The idealized layer of oxygen and associated occupied metal sites, which repeats to form the L–$Li_2Mo_4O_{13}$ model, viewed perpendicular to ($\bar{1}10$). The occupied metal site, A, of the layer above is always positioned directly over the oxygen site, B, of the lower layer. The ordered filling of the metal sites is such that pairs of layers with molybdenum in the metal sites are separated from like pairs by single layers in which lithium fills the metal sites.

close packed layer of oxygen with its associated metal sites, shown in Fig. 1, stacks with identical layers to form the structure. Each layer is related to the identical layer above by a simple translation. That is, the metal site, *A*, always sits directly above the oxygen site, *B*, of the layer below, with the orientation of all layers being the same. Every third layer of metal sites is filled by lithium only, while the first and second layers contain molybdenum only, the sequence of metal layers being:

–Mo–Mo–Li–Mo–Mo–Li–

In terms of metal–oxygen polyhedra this description is equivalent to the stacking of layers composed of isolated groups of four and two edge-sharing octahedra (octahedra 1, 2, 3, 4 and 5′, 6′ in Fig. 2). Each layer is joined to identical layers above and below by shared edges to give a three-dimensional network (Fig. 2) with every pair of molybdenum–oxygen layers being separated by a single layer of lithium–oxygen octahedra. The unoccupied anion sites result in cube–octahedral holes which share faces to form double chains running in the [101] direction through the structure.

Stereoscopic views (*15*) of the molybdenum–oxygen and lithium–oxygen polyhedra are presented in Figs. 3 and 4. The distortion of octahedral coordination around molybdenum towards tetrahedral, and the resulting division of molybdenum–oxygen distances into short, medium and long distances has been noted previously for other molybdenum compounds (*12*, and references cited therein). In L–$Li_2Mo_4O_{13}$ the coordination around each of the six molybdenum atoms in the asymmetric unit shows the

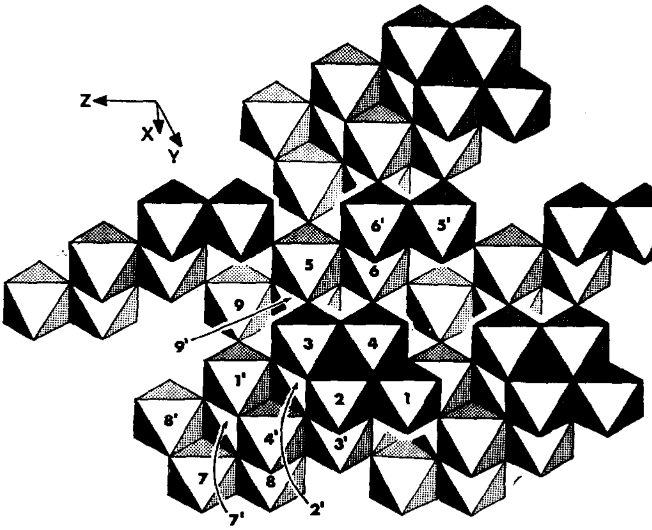

FIG. 2. The idealized structure viewed in the same direction as in Fig. 1. This arrangement of octahedra extends infinitely in three dimensions. Molybdenum and lithium are segregated into layers with every third layer being composed of Li–O octahedra only. Octahedra numbered 1 to 6 correspond to the octahedra about Mo(1) to Mo(6) respectively while octahedra 7, 8 and 9 correspond to the octahedra about Li(1), Li(2) and Li(3). Primes indicate octahedra related by centrosymmetry.

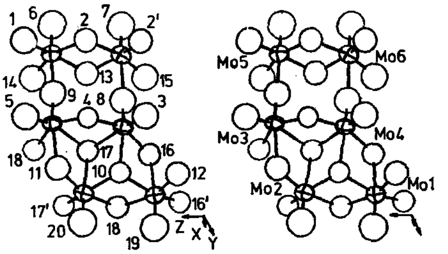

FIG. 3. A stereoscopic view of the six molybdenum atoms in the asymmetric unit and their associated oxygen atoms viewed in the same direction as in the previous figures. The molybdenums are numbered on the right-hand part of the diagram; the numbers on the left-hand part refer to the oxygen atoms.

same tendencies. That is, the major component of the displacement of the molybdenum atom from the centre of the octahedron is always towards an edge. In addition, the octahedral sites are themselves distorted, with the distances between the oxygens defining the edges of the octahedra varying between 2.42 and 3.26 Å. The octahedra of oxygens around the lithium atoms are also distorted, the edge lengths lying between 2.59 and 3.39 Å.

The result of the distortions within the molybdenum coordination polyhedra is that each molybdenum has two short, *cis* oxygen contacts which lie in the narrow range 1.67 to 1.75 Å and two medium distances which are *trans* to each other and vary from 1.89 to 2.04 Å. The remaining two *cis*, long distances comprise one long distance from 2.13 to 2.27 Å and one very long distance from 2.34 to 2.64 Å (Table III). Thus all molybdenum atoms, Mo(6) in particular, show a distinct tendency towards a coordination intermediate between tetrahedral and square-pyramidal. It appears that the distorted octahedra are arranged so that the distances between the molybdenum atoms are maximized. This is reflected in the molybdenum–lithium distances for edge-sharing octahedra which are, on the average, less than the corresponding lithium–lithium and molybdenum–molybdenum distances (Table III).

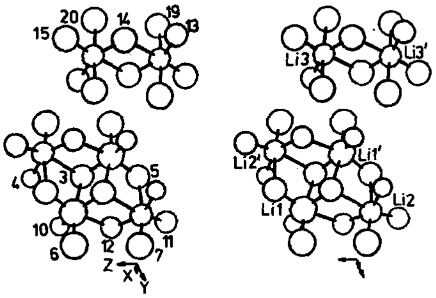

FIG. 4. A stereoscopic view of the lithium and oxygen atoms forming the isolated groups of two and four octahedra, which are the basic unit in the layer of lithium–oxygen octahedra. The lithium atoms are numbered on the right-hand part of the diagram; numbers on the left-hand part refer to oxygens. The unlabelled oxygens are related to those which are labelled by the centres of symmetry apparent from the numbering of the lithiums.

As is usual for molybdenum oxides, the molybdenum–molybdenum distances lie in the range 3.238–3.574 Å for edge-shared octahedra and are somewhat shorter than those for corner-shared octahedra (3.734–4.307 Å). The distance between Mo(4) and Mo(6) is unusually long for corner-shared octahedra and is due to the particularly long Mo(6)–O(8) distance (2.64 Å), the Mo(6) octahedron having a very strong square pyramidal/tetrahedral distortion.

The near-neighbour oxygen–oxygen distances lie in the very broad range 2.42–3.83 Å. The average separation is 2.91 Å although, as might be expected, the distribution of distances has a maximum at about 2.81 Å. The average distance between oxygens forming a shared edge between two molybdenum–oxygen octahedra is 2.58 Å (2.42–2.78 Å) which is shorter than the average for all the edges of molybdenum–oxygen octahedra (2.79 Å). The corresponding value for edges shared between molybdenum–oxygen and lithium–oxygen octahedra is 2.73Å (2.59–2.97Å) and for two lithium–oxygen octahedra, a higher value of 3.04 Å (2.90–3.29 Å). The longest distances are generally those between two oxygens which do not form the edge of any metal–oxygen octahedron.

Discussion

The structure of L–$Li_2Mo_4O_{13}$ is similar to that of $K_2Mo_4O_{13}$ (4) which is the only other tetramolybdate structure known. The molybdenum–oxygen chain formed by the octahedra 1, 2, 3, 4, 1′, 2′, 3′, and 4′ (Fig. 2) is identical to that found in $K_2Mo_4O_{13}$. The relationship of this chain of octahedra to other polymolybdate structures was discussed by Gatehouse and Leverett (*4*). The infinite chain of molybdenum–oxygen and lithium–oxygen octahedra in L–$Li_2Mo_4O_{13}$ (octahedra 1, 2, 3, 4, 7, 8 of Fig. 2

TABLE III

SELECTED INTERATOMIC DISTANCES WITH THEIR ESTIMATED STANDARD DEVIATIONS IN PARENTHESES[a]

Metal–Metal Distances

Mo–Mo edge-shared octahedra	
Mo(1)–Mo(2)	3.252(2)
–Mo(1′)^{a}	3.390(2)
–Mo(4)	3.483(2)
Mo(2)–Mo(3′)	3.238(2)
–Mo(2′)	3.491(2)
–Mo(3)	3.542(2)
–Mo(4)	3.574(1)
Mo(3)–Mo(4)	3.242(2)
Mo(5)–Mo(6)^{a}	3.265(2)
Mo(6)–Mo(6′)^{j}	3.305(2)

Mo–Li edge-shared octahedra	
Mo(1)–Li(1)	3.20(3)
Mo(3)–Li(2)	3.28(3)
Mo(4)–Li(2′)^{b}	3.14(3)
–Li(1)	3.35(3)
Mo(5)–Li(3′)	3.16(3)

Li–Li edge-shared octahedra	
Li(1)–Li(2′)^{b}	3.40(5)
–Li(2)^{a}	3.43(5)
–Li(1′)^{d}	3.56(4)
Li(3)–Li(3′)^{c}	3.37(5)

Mo–Mo corner-shared octahedra	
Mo(1)–Mo(4′)^{a}	3.733(2)
–Mo(3′)	3.962(2)
Mo(2)–Mo(4′)	3.960(2)
Mo(3)–Mo(5)^{c}	4.164(2)
Mo(4)–Mo(6)^{e}	4.307(2)
Mo(5)–Mo(5′)^{i}	3.772(2)
–Mo(6′)^{i}	3.950(2)

Mo–Li corner-shared octahedra	
Mo(1)–Li(2)^{a}	3.65(3)
–Li(3′)	3.89(3)
Mo(2)–Li(2)	3.56(3)
–Li(1)	3.70(3)
–Li(3)^{g}	3.93(3)
Mo(3)–Li(1′)^{b}	3.54(3)
–Li(2′)^{b}	3.64(3)
Mo(4)–Li(1′)^{d}	3.59(3)
Mo(5)–Li(1)	3.61(3)
–Li(3)^{g}	3.68(3)
Mo(6)–Li(3)^{g}	3.61(3)
–Li(2)	3.61(3)
–Li(3′)^{f}	3.71(3)

Metal–Oxygen Distances

Mo–O octahedra

Mo(1)–O(19)	1.68(1)
–O(12)^{a}	1.70(1)
–O(16′)^{a}	1.92(1)
–O(10)	2.04(1)
–O(18′)	2.17(1)
–O(16)	2.34(1)
Mo(2)–O(20)	1.67(1)
–O(11)	1.75(1)
–O(17′)	1.93(1)
–O(10)	1.95(1)
–O(18′)	2.14(1)
–O(17)	2.50(1)

Mo(3)–O(9)	1.70(1)
–O(5)	1.71(1)
–O(4)	1.92(1)
–O(18)	1.92(1)
–O(17)	2.27(1)
–O(11)	2.38(1)
Mo(4)–O(8)	1.67(1)
–O(3)	1.71(1)
–O(4)	1.94(1)
–O(16)	1.98(1)
–O(17)	2.16(1)
–O(10)	2.40(1)

Mo(5)–O(6)	1.70(1)
–O(14)^{g}	1.72(1)
–O(1)^{g}	1.886(1)
–O(13)^{g}	1.98(1)
–O(2)	2.12(1)
–O(9)^{g}	2.47(1)
Mo(6)–O(7)	1.69(1)
–O(15)^{g}	1.70(1)
–O(2′)^{i}	1.90(1)
–O(13)^{h}	1.91(1)
–O(2)^{f}	2.25(1)
–O(8)^{h}	2.64(1)

Li–O octahedra

Li(1)–O(6)	1.91(3)
–O(5′)^{b}	1.93(4)
–O(3′)^{d}	1.96(3)
–O(10)	2.10(3)
–O(5)^{a}	2.56(4)
–O(3)	2.58(3)

Li(2)–O(7)	1.93(3)
–O(11)	1.98(3)
–O(12)	1.99(3)
–O(4′)^{b}	2.02(3)
–O(5)	2.40(3)
–O(3′)^{b}	2.57(3)

Li(3)–O(15)	1.93(3)
–O(14)	2.02(3)
–O(13′)^{c}	2.06(3)
–O(19′)	2.22(3)
–O(20)^{c}	2.27(3)
–O(14′)^{c}	2.46(3)

---

[a] The numbering of the atoms is in accordance with that shown in Table II, with primes indicating atoms in the symmetry related position ($\bar{x}, \bar{y}, \bar{z}$). The superscripts indicate that the atom is in an adjacent unit cell, the relationship of which to the primary unit cell is given by:

a (0, 0, −) c (0, −, 0) e (0, −, −) g (0, +, 0) i (−, +, 0)
b (−, 0, 0) d (−, 0, −) f (0, 0, +) h (0, +, +) j (−, +, +)

and the octahedra related to these by a centre of symmetry) is reminiscent of similar chains found in $Ag_6Mo_{10}O_{33}$ (*12*), the red and blue potassium molybdenum bronzes (*16*, *17*), the caesium molybdenum bronze (*18*) and cobalt molybdate (*19*).

As mentioned previously, L–$Li_2Mo_4O_{13}$ is a regular substitution structure of the V_6O_{13} structure type and as such is another example of the $m=2$, $n=3$ member of the B_1Cm,n and B_2Cm,n groups of oxides proposed by Andersson (*20*, *21*). The relationship of M_6O_{13} to the other members of these groups, particularly the end members of the $m=2$ and $n=3$ series, R–Nb_2O_5(V_2O_5, $W_3V_5O_{20}$) and Nb_3O_7F, was shown by Andersson. The V_6O_{13}(L–$Li_2Mo_4O_{13}$) structure type can be formed by joining ($3\times2\times\infty$) ReO_3 type blocks of octahedra by two mutually perpendicular shear planes. The displacements along the two shear planes are $(\frac{1}{2}\bar{b}+\frac{1}{2}\bar{c})$ and $(\frac{1}{2}\bar{a}+\frac{1}{2}\bar{b})$ respectively; a, b and c being the edges of the ReO_3-type cell with c the direction of infinite extension of the ($3\times2\times\infty$) blocks of octahedra and a the edge 3 octahedra wide. If these shear operations are applied to the ReO_3 model in reverse order a model with M_6O_{13} stoichiometry but a structure different to that of V_6O_{13} is formed. There appears to be no known example of this structure. The direction of infinite corner sharing of octahedra in L–$Li_2Mo_4O_{13}$ is parallel to the [101] direction and corresponds to the b-axis of V_6O_{13} (*14*); the a-axis of V_6O_{13} corresponds to the $[10\bar{1}]$ direction in L–$Li_2Mo_4O_{13}$.

The strong distortions of the Mo–O octahedra in L–$Li_2Mo_4O_{13}$ suggest that Mo^{VI} is very close to the critical size (*22*) for transition from octahedral to lower coordination. For each Mo–O octahedron the existence of two Mo–O separations considerably greater than the sum of the ionic radii for Mo^{6+} and O^{2-} ($0.60+1.40=2.00$ Å, (*23*)), with one of these separations being somewhat longer than the other, would tend to support the idea that there is only a marginal difference between the relative stabilities of octahedral, square pyramidal and tetrahedral coordination. Indeed, the change of composition from the tetramolybdate to the simple molybdate is sufficient to stabilize tetrahedral coordination—Li_2MoO_4 has the phenacite structure. This is similar behaviour to that found in the K_2MoO_4–MoO_3 and Rb_2MoO_4–MoO_3 systems where, as the composition changes from tetramolybdate (*4*) to trimolybdate (*24*), dimolybdate (*25*) and simple molybdate (*26*), the coordination of molybdenum by oxygen changes from octahedral to mixed octahedral and square pyramidal, octahedral and tetrahedral, and finally tetrahedral.

Acknowledgments

This work forms part of a project supported by the Australian Research Grants Committee. One of us (B. K. M.) acknowledges the receipt of a Commonwealth Postgraduate Research Award.

References

1. F. Hoermann, *Z. anorg. u. allgem. Chem.* **177**, 154 (1928).
2. W. S. Brower, H. S. Parker, R. S. Roth, and J. L. Waring, *J. Cryst. Growth* **16**, 115 (1972).
3. M. Parmentier, J. M. Reau, C. Fouassier, and C. Gleitzer, *Bull. Soc. Chim.* 1743 (1972).
4. B. M. Gatehouse and P. Leverett, *J. Chem. Soc.* (A), 2107 (1971).
5. B. M. Gatehouse, D. J. Lloyd, and B. K. Miskin, *Proc. 5th Materials Symp.*, N. B. S. Special Publication No. 364, 15 (1972).
6. L. H. Thomas and K. Umeda, *J. Chem. Phys.* **26**, 293 (1957).
7. D. T. Cromer and J. T. Waber, *Acta Cryst.* **18**, 104 (1965).
8. C. H. Dauben and D. H. Templeton, *Acta Cryst.* **8**, 841 (1955).
9. W. R. Busing, K. O. Martin, and H. A. Levy. ORFLS, a Fortran Crystallographic Least-squares Program. ORNL-TM-305. Oak Ridge National Laboratory, Oak Ridge, Tennessee (1962).
10. R. Shiono (1968). "SF" Block Diagonal Least Squares Refinement Program, Department of Crystallography, University of Pittsburgh, Pa. 15213.
11. J. C. B. White (1965). Melbourne University Fourier Program MUFR3. See Rollet, J. S. "Computing Methods and the Phase Problem in X-ray Crystal Analysis, (Pepinsky, Robertson, and Speakman Eds.), p. 87, Pergamon Press, Oxford (1961).
12. B. M. Gatehouse and P. Leverett, *J. Solid State Chem.* **1**, 484 (1970).
13. M. J. Buerger, *J. Chem. Phys.* **15**, 1 (1947).
14. F. Aebi, *Helv. Chim. Acta* **31**, 9 (1948).
15. C. K. Johnson (1965). ORTEP. ORNL-3794, Oak Ridge National Laboratory, Tennessee.
16. N. C. Stephenson and A. D. Wadsley, *Acta Cryst.* **18**, 241 (1965).
17. J. Graham and A. D. Wadsley, *Acta Cryst.* **20**, 93 (1966).
18. W. G. Mumme and J. A. Watts, *J. Solid State Chem.* **2**, 16 (1970).

19. G. W. Smith and J. A. Ibers, *Acta Cryst.* **19**, 269 (1965).

20. S. Andersson, *Bull. Soc. Chim.* 1088 (1965).

21. S. Andersson, *Arkiv Kemi* **26**, 521 (1967).

22. L. E. Orgel, *Disc. Faraday Soc.* **26**, 138 (1958).

23. R. D. Shannon and C. T. Prewitt, *Acta Cryst.* **B 25**, 925 (1969).

24. B. M. Gatehouse and P. Leverett, *J. Chem. Soc.* (A), 1398 (1968).

25. S. A. Magarill and R. F. Klevtsova, *Sov. Phys. Cryst.* **16**, 645 (1972).

26. B. M. Gatehouse and P. Leverett, *J. Chem. Soc.* (A), 849 (1969).